

УДК 66.067

<https://doi.org/10.37827/ntsh.chem.2022.70.138>

Iryna IVANENKO, Yuriï FEDENKO, Anna STEPANOVA, Olena BYTS

SYNTHESIS OF TITANIUM (IV) OXIDE AND PROSPECTS OF ITS APPLICATION IN ADSORPTION AND PHOTOCATALYTIC WATER TREATMENT PROCESSES

*National Technical University of Ukraine
“Igor Sikorsky Kyiv Polytechnic Institute”,
Peremogy Ave., 37, 03056 Kyiv, Ukraine
e-mail: fedenkoyura@ukr.net*

Pure titanium oxide (TiO₂(ng)) and modified with potassium fluoride with different percentage of dopant: 2, 7, 15% (TiO₂(2F), TiO₂(7F), TiO₂(15F), respectively) samples were synthesized by low-temperature sol-gel method. The morphology and particle size of pure titanium(IV) oxide (TiO₂(ng)) and titanium(IV) oxide doped with potassium fluoride (TiO₂(2F)) were investigated by scanning electron microscopy method. It was found that the doping with potassium fluoride does not have a significant effect on the shape of the particles, but allows to narrow the particle size distribution. X-ray phase and X-ray structural analyzes of the obtained TiO₂ samples showed that the predominant phases of pure TiO₂ were rutile and brookite, and only anatase contained in TiO₂ doped with KF. The porous structure of the synthesized TiO₂ samples was studied by the method of low-temperature nitrogen adsorption-desorption. It was found that the all obtained TiO₂ samples belonged to porous adsorbents, the adsorption of which carried out monolayer. The adsorption properties of the obtained TiO₂ samples were investigated using a model pollutant, phenol. It was found that the best adsorption properties showed TiO₂(2F) sample at all three concentrations of pollutant. The maximum adsorption degree of phenol with an initial concentration of 3.125 mg/dm³ (18%) was achieved by TiO₂(2F) sample; with an initial phenol concentration of 6.25 mg/dm³ was 21.5%, and at an initial phenol concentration of 12.5 mg/dm³ it was 42%. The highest photocatalytic activity was shown by the sample of low-doped fluorine TiO₂, in the presence of which phenol was decomposed by 68%.

Keywords: titanium (IV) oxide, sol-gel method, doping, adsorption, photocatalyst.

Introduction

Titanium (IV) oxide can exist in various allotropic modifications. The most famous natural modifications of TiO₂ are anatase, rutile and brookite. Only the first two crystalline forms are used in industry [1–3].

Among the three modifications, rutile is the most thermodynamically stable form. It is formed from anatase and brookite when heated to a temperature of 600–800 °C, depending on the atmosphere [4, 5]. Anatase and rutile are tetrahedral crystalline systems, while brookite is orthorhombic. In all three modifications, the oxygen atoms are arranged around

the titanium atoms in the form of curved octahedra. In rutile, oxygen atoms have hexagonal dense packing, and in anatase and brookite have cubic dense packing. Half of the octahedral gaps in rutile and the tetrahedral gaps in anatase are occupied by titanium cations. Titanium (IV) oxide is known as a promising adsorbent for the removal of hazardous pollutants from water, in particular phenol [3–10].

Phenol is found in wastewater from the chemical, oil refining, textile, coke-chemical and other industries. It is an extremely dangerous water pollutant, and today there are no universal and effective methods of its removal from waste industrial effluents. Among these methods reagent, extraction and many others are widely used. But they all have certain disadvantages; the need for valuable reagents, incomplete degree of extraction, and most importantly, the need for further disposal of removed phenol. Compared with the above methods, the method of adsorption has significant advantages, which makes it extremely promising and arouses great interest in the scientific world [10–20].

Currently, there is an increasing interest in the use of a photocatalyst based on titanium oxide (TiO₂). Photocatalysis is a fairly inexpensive and easy-to-apply technology capable of solving many problems, while requiring virtually no costs during operation. Photocatalysis requires the catalyst itself (TiO₂), which is not consumed, and sunlight or ultraviolet radiation.

In this regard, the task of new adsorbents and photocatalysts creation and research on the processes of phenol removal in order to select the optimal parameters for their application and development of the technological implementation of these processes into industrial conditions is very relevant.

Materials and Methods

The synthesis of TiO₂ samples was carried out by the modified low-temperature sol-gel method [21]. For this 15wt.% titanium (III) sulfate solution in sulfuric acid was used as a precursor. To it a pre-prepared ammonium hydroxide solution with pH 8 was slowly added dropwise until a pH of 1.2 was reached. In the synthesis of doped samples during the adjustment of the precursor solution to pH 1.2 a portion of pre-weighed KF (according to table 1) was added in several small portions. After reaching a pH of 1.2, the solution was heated to a temperature of 50 °C with constant stirring to undergo low-temperature hydrolysis for 30 minutes. Data for the synthesis of titanium (IV) oxide doped with potassium fluoride are presented in Table 1.

Table 1

Data for the synthesis of titanium (IV) oxide doped with potassium fluoride

№	Sample	Precursor volume, cm ³	Mass of KF, g
1	TiO ₂ (2F)	10	0.300
2	TiO ₂ (7F)	10	0.084
3	TiO ₂ (15F)	10	0.040

After completion of the low-temperature hydrolysis step, the beaker was covered and left for aging during 7 days. Then the obtained precipitate of titanium (IV) oxide was washed on a vacuum filter until the qualitative reaction on SO₄²⁻ ions disappeared, dried in an oven at 60–70 °C for 2 hours, ground in an agate mortar, and placed into a hermetic container for further storage.

Adsorption and photocatalytic decomposition of phenol.

Investigations of the adsorption and photocatalytic properties of the synthesized titanium(IV) oxide samples were performed on a model solution of phenol with the initial concentration of 12.5; 9.375; 6.25; 3.125 mg/dm³.

To study the photocatalytic properties of the synthesized samples of titanium(IV) oxide, an installation with a UV lamp with a power of 24 W and a wavelength of 254 nm was used.

Results and Discussion

Investigation of surface morphology of the TiO₂ samples

The morphology and particle size of pure titanium (IV) oxide (TiO₂(ng)) and titanium (IV) oxide (TiO₂(2F)) samples doped with potassium fluoride were investigated using scanning electron microscopy. The obtained images are presented in Fig. 1.

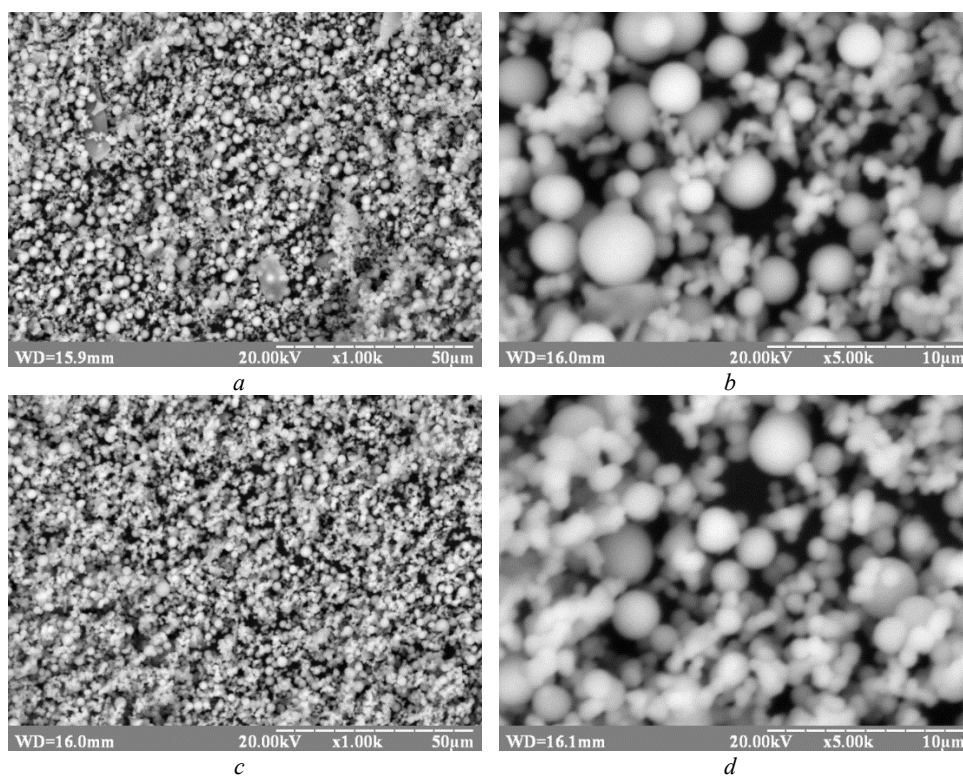


Fig. 1. SEM images of the synthesized TiO₂ samples. *a, b* – TiO₂(ng); *c, d* – TiO₂(2F).

Fig. 1 shows that the particles of both synthesized samples have a spherical shape; their size is in the range of 15–35 μm for TiO₂(ng) and 20–30 μm for TiO₂(2F). This indicates that the addition of potassium fluoride does not have a significant effect on the shape of the particles, but allows to narrow the particle size distribution.

X-ray phase and X-ray structural analysis

Diffractograms of four synthesized TiO₂ samples obtained by X-ray phase analysis are shown in Fig. 2.

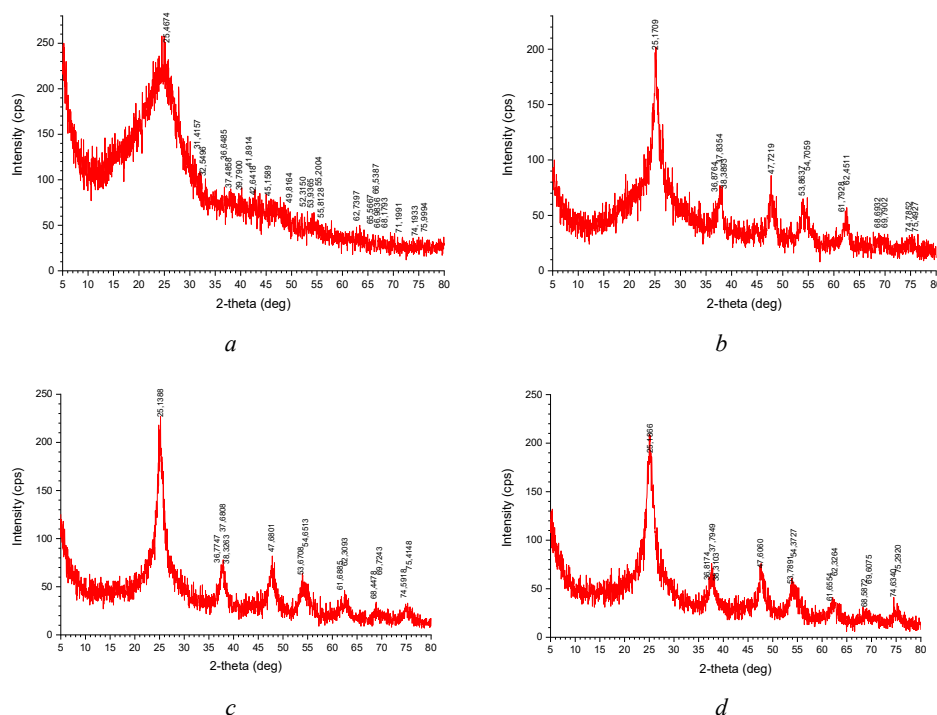


Fig. 2. Diffractograms of synthesized TiO₂ samples.
a – TiO₂(ng); *b* – TiO₂(2F); *c* – TiO₂(7F); *d* – TiO₂(15F).

According to the diffractograms shown in Fig. 2, the TiO₂(ng) sample contains modifications of rutile and brookite, and the other three samples have the structure of pure anatase. These findings were obtained using standard cards of International Center of Diffraction Data № 00-015-0875 (brookite), №00-021-1272 (anatase), №00-021-1276 (rutile).

Crystallograms of the TiO₂ samples obtained by X-ray structural analysis are shown in Fig. 3.

As can be seen from the crystallograms shown in Fig. 3, in the TiO₂(ng) sample there are (110), (111), (002), (200), (220), (202), (221) planes of rutile, and (112), (022), (113), (132) planes of brookite. In the TiO₂(2F), TiO₂(7F), TiO₂(15F) samples there are (101), (103), (004), (112), (200), (105), (211), (213), (204), (116), (220), (215), (301) planes, which are inherent in the structure of anatase. These findings were obtained using standard cards of International Center for Diffraction Data № 00-015-0875 (brookite), № 00-021-1272 (anatase), № 00-021-1276 (rutile).

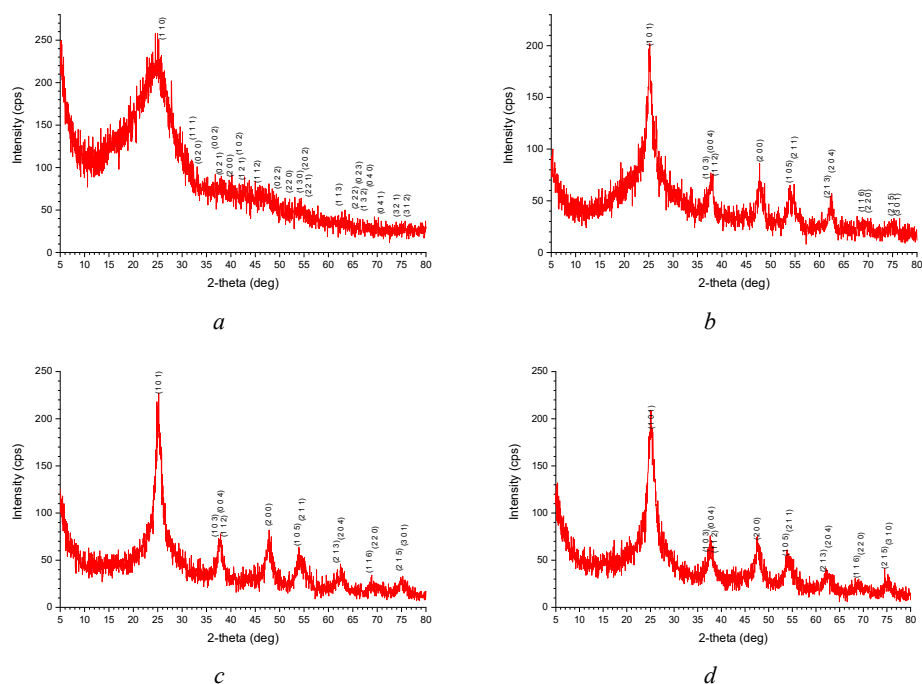


Fig. 3. Crystallograms of synthesized TiO_2 samples.
 a – $\text{TiO}_2(\text{ng})$; b – $\text{TiO}_2(2\text{F})$; c – $\text{TiO}_2(7\text{F})$; d – $\text{TiO}_2(15\text{F})$.

While processing the results of X-ray phase analysis, the crystal lattice constants were calculated; they are shown in Table 2.

Table 2

Crystal lattice constants of the synthesized TiO_2 samples

Sample	$a, \text{Å}$	$b, \text{Å}$	$c, \text{Å}$	α	β	γ
$\text{TiO}_2(\text{ng})$	4.527	5.497	4.900	90.00	90.00	90.00
$\text{TiO}_2(2\text{F})$	3.808	3.808	9.503	90.00	90.00	90.00
$\text{TiO}_2(7\text{F})$	3.812	3.812	9.541	90.00	90.00	90.00
$\text{TiO}_2(15\text{F})$	3.817	3.817	9.513	90.00	90.00	90.00

For the $\text{TiO}_2(\text{ng})$ sample, the three faces of the crystal lattice differ in length and indicate a rhombic syngony which is characteristic of brookite. The other three samples have two faces of the same length, so we can conclude that there is a tetragonal syngony, which is characteristic of the modification of anatase.

Low-temperature adsorption-desorption of nitrogen

The curves obtained by the method of low-temperature nitrogen adsorption-desorption on the obtained TiO_2 samples are shown in Fig. 4. The presented isotherms

belong to I type isotherms of gas adsorption on the surface of solids according to the Brunauer classification. They are characteristic of porous adsorbents on which the adsorption is monolayer, and sometimes does not reach the plateau.

The presence of a hysteresis loop in the range of p/p_s from 0–0.1 to 1.0 indicates the availability of mesopores (2–50 nm) in the synthesized samples. It is a noticeable expansion of the hysteresis loop with increasing of fluorine content in the samples. It depends on the curvature of the «saddle», the curvature of the spherical meniscus of the throat pores, as well as their change during the formation of the adsorption layer. The larger the difference in curvature, the wider the hysteresis loop, and for cylindrical pores closed on one side, the adsorption and desorption curves coincide. In $\text{TiO}_2(\text{ng})$ and $\text{TiO}_2(15\text{F})$ samples the adsorption and desorption curves practically coincide, so the hysteresis loop is almost invisible.

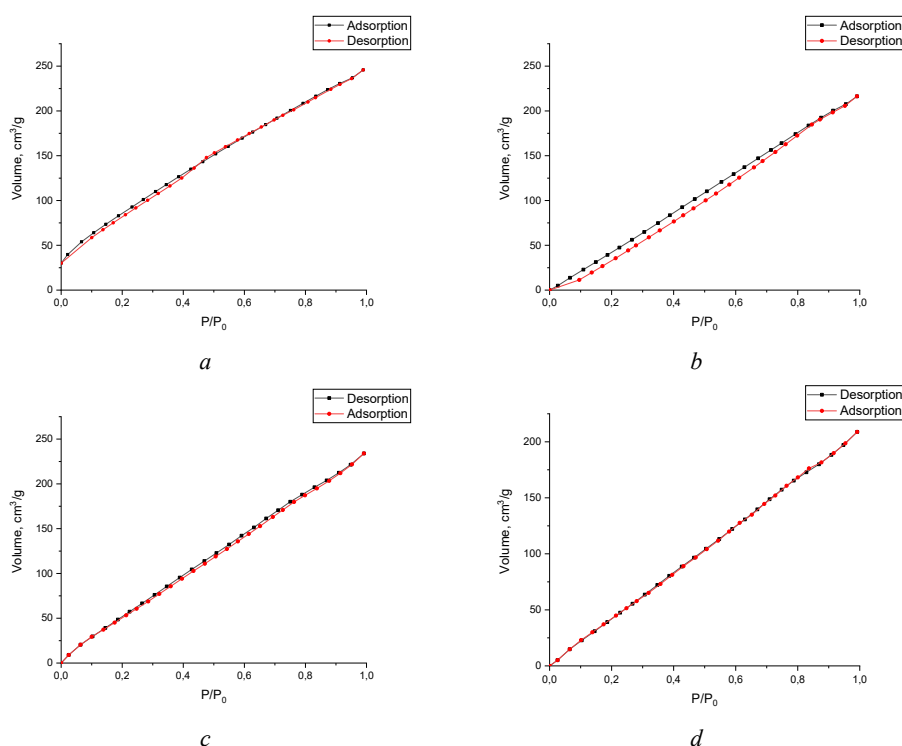


Fig. 4. Nitrogen adsorption-desorption isotherms on the synthesized TiO_2 samples. a – $\text{TiO}_2(\text{ng})$; b – $\text{TiO}_2(2\text{F})$; c – $\text{TiO}_2(7\text{F})$; d – $\text{TiO}_2(15\text{F})$.

The curves of the distribution of the pores by radii derived from the adsorption-desorption isotherms described above are shown in Fig. 5.

Pore distribution curves by radius for the sample of $\text{TiO}_2(\text{ng})$ indicate the presence of mesopores in the sample and an insignificant number of micropores (Fig. 5,a). The porosity of the samples doped with fluorine is slightly lower than that of undoped TiO_2

(Fig. 5,b–d). They have an insignificant, almost equal number of micro- and mesopores, which is reflected in the total porosity of these catalysts, as will be shown in the Table 3.

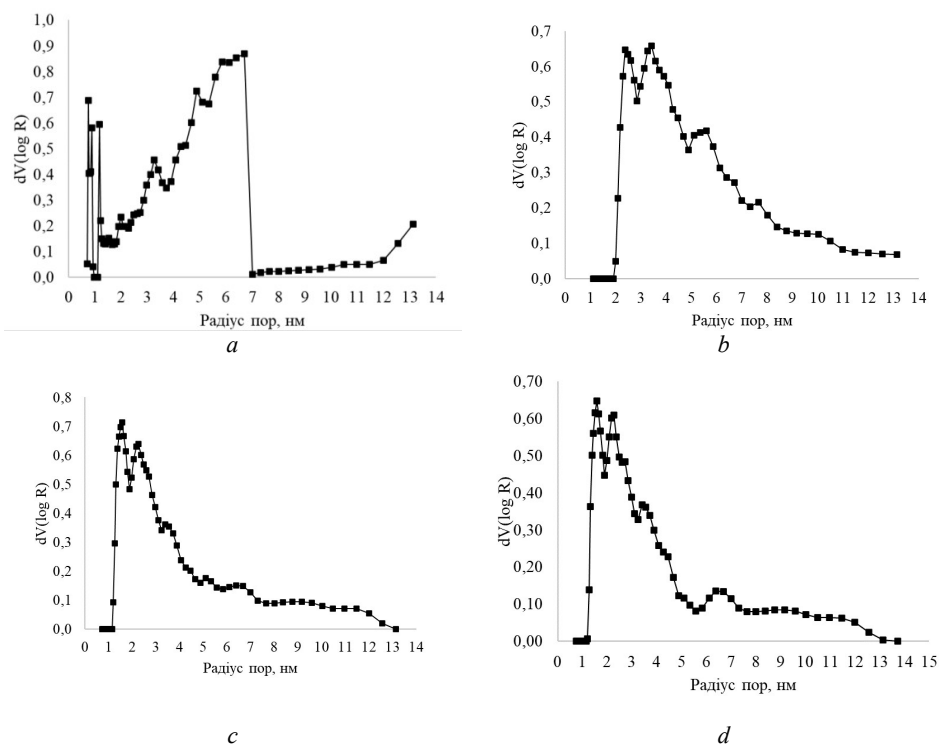


Fig. 5. Pore distribution curves in the synthesized TiO₂ samples.
a – TiO₂(ng); b – TiO₂(2F); c – TiO₂(7F); d – TiO₂(15F).

Structural and adsorption characteristics of the synthesized samples, calculated on the basis of the obtained isotherms of low-temperature nitrogen adsorption-desorption, are shown in Table 3.

Table 3

Structural adsorption characteristics of the synthesized TiO ₂ samples				
Sample	$S_{spec}, m^2/g$	$V_{\Sigma}, cm^3/g$	$V_{micropores}, m^3/g$	D_{por}, nm
TiO ₂ (ng)	67	0.27	0.26	3
TiO ₂ (2F)	53	0.33	0.21	3
TiO ₂ (7F)	55	0.33	0.23	3
TiO ₂ (15F)	49	0.30	0.20	3

According to Table 3, the synthesized samples have a small specific surface area and a small pore volume and total porosity accordingly. The pore diameter is 3 nm, which confirms the presence of mesopores.

Phenol adsorption

The experimental data obtained while a study of the phenol adsorption by the synthesized TiO_2 samples are shown in Fig. 6.

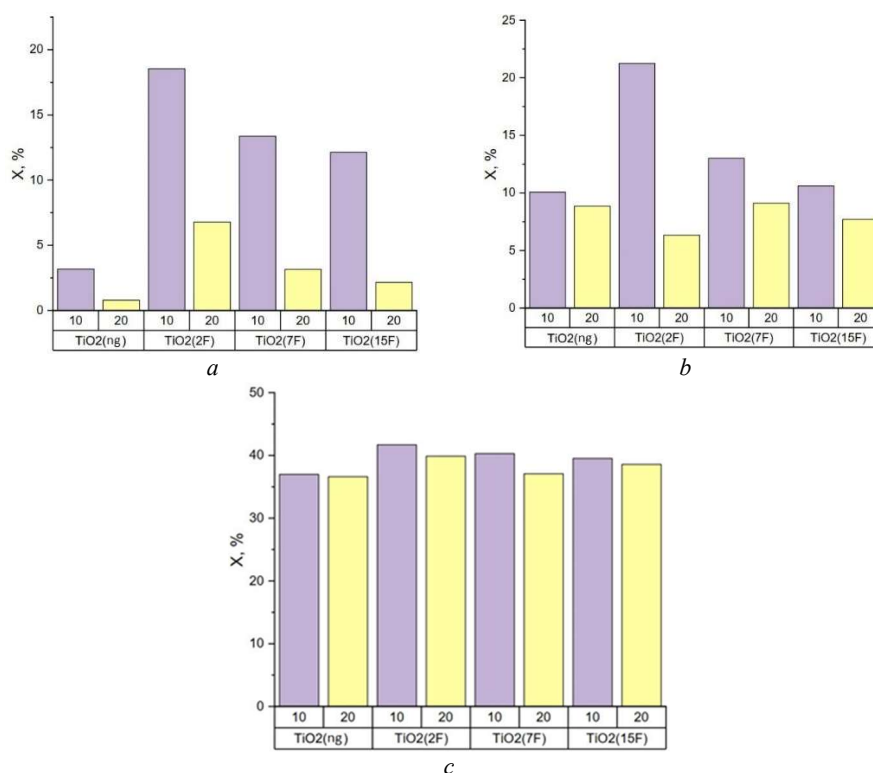


Fig. 6. The adsorption degree of phenol of different initial concentration (a – $C_0 = 3.125 \text{ mg/dm}^3$; b – $C_0 = 6.25 \text{ mg/dm}^3$; c – $C_0 = 12.5 \text{ mg/dm}^3$) on the synthesized TiO_2 samples.

The histograms of Fig. 6 show an increase in the degree of phenol adsorption from solution with the initial concentration of pollutant increasing. The adsorption of the pollutant may increase with increasing the adsorption capacity of the synthesized samples. This occurs when the adsorbate molecules are reoriented relative to the surface of titanium (IV) oxide. Because the phenol molecule contains a benzoic ring, its parallel and perpendicular orientation can occur. Another reason for the increase in adsorption capacity may be the rapid transition to polymolecular adsorption. Phenol molecules are adsorbed on the surface of the synthesized samples in the first 10 minutes. Over the next 10 minutes, the phenomenon of pollutant desorption from titanium (IV) oxide is observed.

$\text{TiO}_2(2\text{F})$ sample showed the best adsorption properties at all three pollutant concentrations. The maximum degree of phenol adsorption with an initial concentration of 3.125 mg/dm^3 by the $\text{TiO}_2(2\text{F})$ sample was 18%, with an initial concentration of 6.25 mg/dm^3 – 21.5%, and at a phenol concentration of 12.5 mg/dm^3 it was 42%.

The adsorption properties of the synthesized samples are improved by increasing the fluorine content in the synthesized samples.

The isotherms of phenol adsorption by the synthesized TiO_2 samples obtained in 20 minutes are given in Fig. 7. They have a similar character of concave curves, which confirms the poorly developed microporosity of all obtained photocatalysts, and, as a result, their low adsorption capacity.

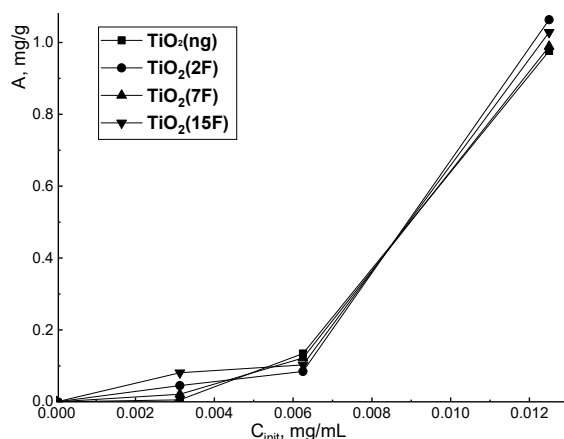


Fig. 7. Phenol adsorption isotherms by the synthesized TiO_2 samples.

Photocatalytic degradation of phenol

The experimental results obtained while a study of the photocatalytic degradation of phenol are shown in Fig. 8.

The degree of photocatalytic decomposition of phenol rises with the increase in the duration of UV irradiation on the pollutant solution, and with the increase in its initial concentration, as can be seen from the histograms in Fig. 8. For example, the degree of photocatalytic decomposition at the duration of UV irradiation of 20 min in the presence of the $\text{TiO}_2(15\text{F})$ sample was 25; 38; 24; 47% and depended on the initial concentration of the pollutant solution.

The highest degree of photocatalytic decomposition of phenol was reached at its initial concentration 12.5 mg/dm^3 in the presence of the $\text{TiO}_2(2\text{F})$ sample and constituted 68%.

Fig. 9 shows the spectra of the initial phenol solution and the phenol solution after photocatalytic degradation.

The spectra of phenol measured before and after the photocatalytic process differ as is seen from the data in Fig. 9. The intensity of the phenol spectrum maxima in the range of 350-400 nm greatly increases after ultraviolet irradiation, which indicates the decomposition of the pollutant and the emergence of new substances, some products of phenol degradation.

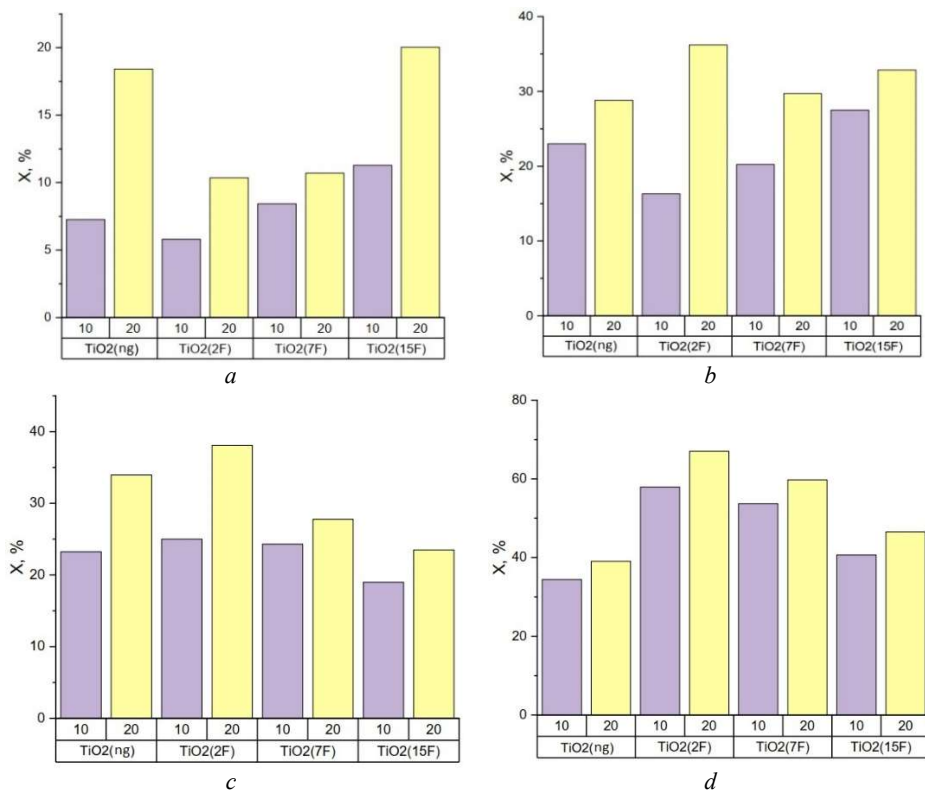


Fig. 8. Photocatalytic degradation of phenol of different initial concentration (a – C₀=3.125 mg/dm³; b – C₀=6.25 mg/dm³; c – C₀=9.375 mg/dm³; d – C₀=12.5 mg/dm³) in the presence of the synthesized TiO₂ samples.

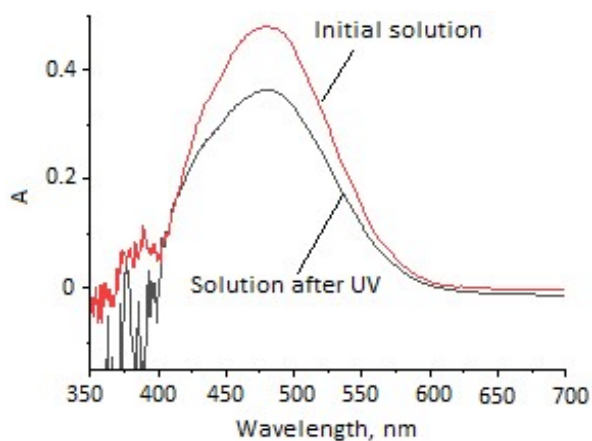


Fig. 9. Spectra of phenol solution before and after photocatalytic degradation.

Conclusions

1. Particles of the samples TiO₂(ng) and TiO₂(2F) synthesized by low-temperature sol-gel method have a spherical shape; their size is in the range of 15–35 μm for TiO₂(ng) and 20–30 μm for TiO₂(2F). This indicates that the addition of potassium fluoride does not have a significant effect on the shape of the particles, but allows to narrow the particle size distribution.
2. Sample TiO₂(ng) contains modifications of rutile and brookite, and the other three samples of TiO₂ supplemented with fluorine have the structure of anatase.
3. Nitrogen adsorption isotherms on all synthesized samples belong to the first type according to the Brunauer classification. They are characteristic of porous adsorbents, the adsorption of which is monolayer, and does not reach the plateau sometimes, have a small specific surface area, and, accordingly, a small pore volume and total porosity. The pore diameter of all TiO₂ samples is 3 nm, which confirms the presence of mesopores.
4. The sample of TiO₂(2F) showed the best adsorption properties toward phenol. The maximum adsorption degree of phenol with an initial concentration of 3.125 mg/dm³ was 18%, with an initial concentration of 6.25 mg/dm³ it equaled 21.5%, and it was 42% at a phenol concentration of 12.5 mg/dm³.
5. The degree of photocatalytic degradation of phenol of all its studied initial concentrations in the presence of TiO₂ synthesized samples exceeded the adsorption degree. The highest photocatalytic activity was shown by the sample of low-doped fluorine TiO₂, in the presence of which phenol was decomposed by 68%.

REFERENCES

1. *Novopysmennyi S.A.* The innovative approaches to creation of health saving environment in educational establishments. P. 16–18. (in Ukrainian). (<http://techno.pnpu.edu.ua/zbirnykBGD17.pdf>).
2. *Ola O., Maroto-Valer M.* Review of material design and reactor engineering on TiO₂ photocatalysis for CO₂ reduction. *J. Photochem. Photobiol. C: Photochem. Rev.* 2015. Vol. 24. P. 16–42. (<https://doi.org/10.1016/j.jphotochemrev.2015.06.001>).
3. *Sharmila Devi R. Venckatesh Dr.R., Rajeshwari Sivaraj Dr.* Synthesis of Titanium Dioxide Nanoparticles by Sol-Gel Technique. *Int. J. Innov. Res. Scie. Eng. Tech.* 2014. Vol. 3. P. 15206–15211. (<https://doi.org/10.15680/IJIRSET.2014.0308020>).
4. *Chen X., Mao S.* Titanium Dioxide Nanomaterials: Synthesis, Properties, Modifications, and Applications. *Chem. Rev.* 2007. Vol. 7. P. 2891–2959. (<https://doi.org/10.1021/cr0500535>).
5. *Hanaor D., Sorrell C.* Review of the anatase to rutile phase transformation. *J. Mat. Scie.* 2011. Vol. 46. P. 855–874. (<https://doi.org/10.1007/s10853-010-5113-0>).
6. *Chen X. Liu L., Yu P., Mao S.* Increasing Solar Absorption for Photocatalysis with Black Hydrogenated Titanium Dioxide Nanocrystals. *Scie.* 2011. Vol. 331. P. 746–750. (<https://doi.org/10.1126/science.1200448>).
7. *Zhang F., Shi F., Ma W., Gao F., Jiao Y., Li H., Wang J., Shan X., Lu X., Meng S.* Controlling Adsorption Structure of Eosin Y Dye on Nanocrystalline TiO₂ Films for Improved Photovoltaic Performances. *J. Phys. Chem.* 2013. Vol. 117 P. 14659–14666. (<https://doi.org/10.1021/jp404439p>).

8. Haider A.J., Al-Anbari R.H. Exploring potential Environmental applications of TiO₂ Nanoparticles. *Energ. Proc.* 2017. Vol. 119. P. 332–345. (<https://doi.org/10.1016/j.egypro.2017.07.117>).
9. Kandiel T.A., L. Robben, Alkaimad A. Brookite versus anatase TiO₂ photocatalysts: phase transformations and photocatalytic activities. *Photochem. Photobiol. Sci.* 2013. Vol. 12. P. 602–609. (<https://doi.org/10.1039/C2PP25217A>).
10. Ehsani A., Adeli S., Babaei F. Electrochemical and optical properties of TiO₂ nanoparticles/poly tyramine composite film. *J. Electroanal. Chem.* 2014. Vol. 713. P. 91–97. (<https://doi.org/10.1016/j.jelechem.2013.12.003>).
11. Staudt J. Synthese, Charakterisierung und optoelektronische Anwendungen von Nb-TiO₂. Doctoral Thesis. 2019 (in German). (<https://doi.org/10.22028/D291-31015>).
12. Winkler J. Titanium dioxide: production, properties and effective use. Hannover: Vincentz Network, 2013. 415 p. (in German).
13. Riedel E., Janiak C. Inorganic chemistry (De Gruyter studies). Berlin: Walter De Gruyter GmbH, 2015. 386 p. (in German).
14. Tekin D., Birhan D., Kiziltas H. Thermal, photocatalytic, and antibacterial properties of calcinated nano-TiO₂/polymer composites. *Mat. Chem. Phys.* 2020. Vol. 1. P. 88–95. (<https://doi.org/10.1016/j.matchemphys.2020.123067>).
15. Modes T. Structure and properties of TiO₂ layers deposited by reactive plasma-activated electron beam evaporation. Diss. 2006. (in German). (<https://doi.org/10.1016/j.surfcoat.2005.02.080>).
16. Kamaruddin S. TiO₂ coatings for the production of photocatalytically modified SiO₂-TiO₂ composite materials. Diss. 2015. (in German).
17. Tian Y., Zhang J. Monodisperse rutile microspheres with ultrasmall nanorods on surfaces: Synthesis, characterization, luminescence, and photocatalysis. *J. Coll. Interf. Sci.* 2012. Vol. 385. P. 1–7. (<https://doi.org/10.1016/j.jcis.2012.06.086>).
18. Anpo M., Kamat P.V. Environmentally Benign Photocatalysts: Applications of Titanium Oxide-based Materials. New York: Springer. 2010. 757 p. (<https://doi.org/10.1007/978-0-387-48444-0>).
19. Landmann M., Rauls E., Schmidt W.G. The electronic structure and optical response of rutile, anatase and brookite TiO₂. *J. Phys.: Condens. Matter.* 2012. Vol. 24. P. 1–6. (<https://doi.org/10.1088/0953-8984/24/19/195503>).
20. Hashimoto K., Irie H. TiO₂ Photocatalysis: A Historical Overview and Future Prospects. *Jap. J. Appl. Phys.* 2005. Vol. 44. P. 8269–8285. (<https://doi.org/10.1143/JJAP.44.8269>).
21. Ivanenko I.M., Kukh A.A., Byts O.V., Astrelin I.M. Synthesis and Adsorption Activity of TiO₂/Activated Carbon Composites / Ed. G. Neeraja Rani, J. Anjaiah, P. Raju. Hamburg, Germany: American Institute of Physics Publishing. 2020. Vol. 2269(1). P. 030–099. (<https://doi.org/10.1063/5.0019932>).
22. Kukh A.A., Ivanenko I.M., Astrelin I.M. TiO₂ and its composites as effective photocatalyst for glucose degradation processes. *Applied Nanoscience.* 2019. Vol. 9. P. 677–682. (<https://doi.org/10.1007/s13204-018-0691-2>).

SUMMARY

Ірина ІВАНЕНКО, Юрій ФЕДЕНКО, Анна СТЕПАНОВА, Олена БИЦЬ

СИНТЕЗ ТИТАН (IV) ОКСИДУ ТА ПЕРСПЕКТИВИ ЙОГО ЗАСТОСУВАННЯ В АДСОРБЦІЙНИХ І ФОТОКАТАЛІТИЧНИХ ВОДОЧИСТИХ ПРОЦЕСАХ

*Національний технічний університет України
«Київський політехнічний інститут імені Ігоря Сікорського»,*

*корп. 4, пр. Перемоги, 37, 03056 Київ, Україна
e-mail: fedenkoyura@ukr.net*

Синтезовано зразки фотокаталізатора на основі титан(IV) оксиду – чистого ($\text{TiO}_2(\text{нг})$) та модифікованого KF із різним відсотковим вмістом допанта: 2, 7, 15% ($\text{TiO}_2(2\text{F})$, $\text{TiO}_2(7\text{F})$, $\text{TiO}_2(15\text{F})$, відповідно) методом низькотемпературного гідролізу. Морфологія та розмір частинок зразків чистого титан(IV) оксиду ($\text{TiO}_2(\text{нг})$) та титан (IV) оксиду ($\text{TiO}_2(2\text{F})$), допованого фторидом калію, досліджено із застосуванням методу скануючої електронної мікроскопії. Встановлено, що допування фторидом калію не має значного впливу на форму частинок, але дозволяє звизити розподіл частинок за розмірами. Проведено рентгено-фазовий та рентгено-структурний аналізи одержаних зразків TiO_2 та встановлено, що переважними фазами у зразку чистого TiO_2 є рутил та брукіт, а при його допуванні KF – анатаз. Встановлено, що в зразку $\text{TiO}_2(\text{нг})$ присутні грані (110), (111), (002), (200), (220), (202), (221) від рутилу, а також грані (112), (022), (113), (132) від брукіту. У зразках $\text{TiO}_2(2\text{F})$, $\text{TiO}_2(7\text{F})$, $\text{TiO}_2(15\text{F})$ присутні грані (101), (103), (004), (112), (200), (105), (211), (213), (204), (116), (220), (215), (301), що притаманні структурі анатазу. Дані висновки були отримані з використанням стандартних карток International Centre for Diffraction Data №00-015-0875 (для брукіту), №00-021-1272 (для анатазу), №00-021-1276 (для рутилу). Досліджено структуру поверхні синтезованих зразків TiO_2 методом низькотемпературної адсорбції-десорбції азоту. Виявлено, що всі одержані зразки TiO_2 належать до поруватих адсорбентів, адсорбція на яких є моношаровою. Адсорбційні властивості отриманих зразків TiO_2 досліджено на прикладі фенолу. Виявлено, що найкращі адсорбційні властивості проявив зразок $\text{TiO}_2(2\text{F})$ за всіх трьох досліджених концентрацій політанту. Максимальний ступінь адсорбційного вилучення зразком $\text{TiO}_2(2\text{F})$ фенолу з вихідною концентрацією $3,125 \text{ мг/дм}^3$ становив 18%, з вихідною концентрацією фенолу $6,25 \text{ мг/дм}^3$ – 21,5%, а при вихідній концентрації фенолу $12,5 \text{ мг/дм}^3$ він становив 42%. Найвищу фотокаталітичну активність показав зразок низькодопованого фтором TiO_2 , у присутності якого фенол розкладався на 68%.

Ключові слова: титан (IV) оксид, золь-гель метод, допування, адсорбція, фотокаталізатор.

Стаття надійшла 10.05.2022.
Після доопрацювання 12.07.2022.
Прийнята до друку 30.09.2022.